Anatomical Insight and Injection Guideline of the Orbicularis Oculi Muscle Using Ultrasonography and Sihler's Staining

Piao, Jiong-Zhen

Department of Applied Life Science
Graduate School
Yonsei University

Anatomical Insight and Injection Guideline of the Orbicularis Oculi Muscle Using Ultrasonography and Sihler's Staining

Advisor Kim Hee-Jin

A Dissertation Submitted
to the Department of Applied Life Science
and the Committee on Graduate School
of Yonsei University in Partial Fulfillment of the
Requirements for the Degree of
Doctor of Philosophy

Piao, Jiong-Zhen

June 2025

Anatomical Insight and Injection Guideline of the Orbicularis Oculi Muscle Using Ultrasonography and Sihler's Staining

This Certifies that the Dissertation of Piao, Jiong-Zhen is Approved

Committee Chair	**Kim, Hee-Jin**
Committee Member	**Hu, Kyung-Seok**
Committee Member	**Jung, Han-Sung**
Committee Member	**Gil, Young-Chun**
Committee Member	**Choi, You-Jin**

Department of Applied Life Science
Graduate School
Yonsei University
June 2025

ACKNOWLEDGEMENTS

Time has flown by, and in the blink of an eye, four years have passed since I arrived in this country and became a part of this exceptional lab team. Coming to a foreign land and navigating an unfamiliar environment, I have faced numerous challenges and overcome many obstacles, all of which have shaped my growth. On this outstanding platform, my understanding of scientific research has grown richer and more multifaceted. I have come to realize that the expansion of the field of anatomy is brimming with boundless creativity and potential.

First and foremost, I wish to extend my deepest respect to those who donated their bodies and to their families. Their noble spirit has profoundly contributed to the advancement of science, and they stand as the very first teachers of all medical students and researchers.

My advisor, Professor Hee-Jin Kim, possesses unparalleled passion for research and exceptional perceptiveness in judgment. I am deeply grateful for his generous guidance and invaluable advice. His demeanor and spirit, both as a scholar and an advisor, have earned my respect and admiration. Additionally, I am profoundly grateful to Professor Kyung-Seok Hu for the unwavering support and patience in helping me clarify my doubts during my time in the laboratory. It has been an immense honor to be a student under the guidance of both esteemed professors.

I also wish to thank Professor Han-Sung Jung and Professor Young-Chun Gil for their valuable suggestions during the writing process of my dissertation, helping me identify and correct its shortcomings. My heartfelt gratitude also goes to Mr. Min-Kyu Kang, who has quietly dedicated himself to the laboratory, taking care of each of us with great thoughtfulness and care.

I would like to express my heartfelt gratitude to all my colleagues in the laboratory. My special thanks go to Professor You-Jin Choi, the most experienced colleague, for the care and support that helped me quickly adapt to the team. I am deeply grateful to Professor Hyung-Jin Lee for the incisive and insightful advice on academic matters. I also extend my gratitude to Professors Ji-Hyun Lee and Kang-Woo Lee, whose abundant creativity provided numerous outstanding suggestions that greatly helped my experimental process. I am deeply grateful to Professor Kyu-Lim Lee. She has consistently provided me with thoughtful guidance and practical advice, helping me stay on track and plan effectively. My appreciation also goes to Professor Hyungkyu Bae, Professor Hyun-Jin Park, and Dr. Hyo-Sang An for their support during my doctoral journey, which greatly enriched my laboratory

experience. I am sincerely grateful to Ms. Hye-Won Hu, who has patiently provided exquisite illustrations for my papers throughout this journey. I also extend my thanks to Professor Soo-Bin Kim and Ms. Hae-Ryun Ahn for actively helping me share the responsibilities of lab tasks. I also want to extend my gratitude to Ms. Yuyoung Kim, who actively reminded me of specific details at every stage of the thesis submission process. Having recently overcome cancer, her boundless enthusiasm and unwavering courage will undoubtedly pave the way for her future success. I am thankful to Professor Yu-Ran Heo, Mr. Kyeong-Sik Yoon, Ms. Goun Jung, and Ms. Ju-Hyun Kim, who have recently joined the team and injected it with vibrant and dynamic energy. I also want to acknowledge Ms. Hyun-Ju Ji and Ms. Su-Jeong Kim share brief but memorable moments with the team. I wish you both a speedy return.

And my girlfriend, who has stood by my side and supported me through our time in a foreign land. Your care and support have allowed me to feel the warmth of home even in an unfamiliar environment. Finally, I want to thank my mother, father, grandmother, and paternal grandmother for their unwavering support and constant care. With few words but immense actions, you have made the greatest sacrifices for me. I am profoundly grateful for everything you have done.

Over these four years, my mindset and outlook on life have undergone profound transformations. I have experienced moments of boundless passion and unwavering ambition, yet I have also faced periods of uncertainty, self-doubt, and an inexplicable sense of solitude. This cycle of emotions seemed to repeat itself, as though the self-reflection inherent in personal growth is a journey without a definitive conclusion. Perhaps, true growth lies in the ability to embrace and confront a self that is constantly being redefined. This was the most treasured and profound realization that my doctoral journey has given me.

TABLE OF CONTENT

LIST OF FIGURES

LIST OF TABLES

ABSTRACT

Anatomical Insight and Injection Guideline of the Orbicularis Oculi Muscle Using Ultrasonography and Sihler's Staining

The orbicularis oculi muscle (OOc) is an elliptically broad and flattened muscle that is strongly associated with facial aging as its contraction causes the formation of crow's feet. The botulinum toxin (BoNT) is one of the representative treatments targeting OOc. This study's aim was to demonstrate the anatomical information of the OOc self, including muscle width, thickness, dynamic features and anatomical relationship between the OOc and zygomaticus complex muscles using ultrasonography, as well as to visualize the distribution of the facial nerve that innervates the OOc using Sihler's staining, thereby providing reference data for BoNT injection targeting OOc.

Twenty healthy Korean volunteers participated. The width, thickness, and dynamic movement of the OOc were measured on horizontal plane using ultrasonography. The positional relationship and overlapping ranges between the OOc, zygomaticus minor (Zmi), zygomaticus major (ZMj), as well as their distances from the skin, were measured on four different perpendicular planes using ultrasonography. And the modified Sihler's staining was conducted on specimens of the OOc.

At the lateral canthus horizontal plane (LCHP), the distance between the lateral margin of the frontal process of zygomatic bone and the most lateral margin of the OOc was 12.5 ± 1.3 mm. The depth of the OOc at the midpoint of the frontal process, the lateral marginal of the frontal process, and 5 mm lateral to the frontal process was 2.0 ± 0.4 mm, 2.8 ± 0.4 mm, and 3.1 ± 0.5 mm. The thicknesses of the OOc at the midpoint of the frontal process, the lateral marginal of the frontal process, and 5 mm lateral to the frontal process were 0.7 ± 0.3 mm, 1.1 ± 0.3 mm, and 1.2 ± 0.3 mm.

The mean distances between the LCHP and the zygomaticus complex muscles superior margin were 20.0 mm, 17.9 mm, 22.8 mm and 20.8 mm at perpendicular plane lateral canthus, orbital rim, midpoint of the frontal process of zygomatic bone and jugale point. The mean distances between the OOc and skin were 4.9 mm, 4.8 mm, 5.5 mm and 4.7 mm at each perpendicular plane. The mean distances between the zygomaticus complex muscles and OOc were 3.0 mm, 3.1 mm, 4.5 mm and 4.1 mm at each perpendicular plane.

The author proposed new insights for crow's feet injection based on anatomical

information obtained from ultrasonography and Sihler's staining which would contribute to minimizing complications and improving effect during the administration of BoNT.

Key words: Orbicularis oculi muscle, Ultrasonography, Sihler's staining, Crow's feet, Botulinum toxin.

1. Introduction

The orbicularis oculi muscle (OOc) is an elliptically broad and flattened muscle that is involved in a range of facial expressions.[1] This involvement stems from its overlaps with neighboring muscles to which it is directly or indirectly connected.[2] The OOc consists of three parts, delineated based on their location: pretarsal, preseptal, and orbital part. The orbital part is strongly associated with facial aging as its contraction causes the formation of crow's feet. When the OOc is active, the skin of the lateral orbit is drawn toward the medial side, and skin wrinkles are formed due to the contraction of the OOc. Noticeable crow's feet are among the most common signs of facial aging.[3]

Previous studies suggest that the point at which botulinum toxin (BoNT) is injected for crow's feet on the OOc should be located 1.5-2.0 cm lateral to the lateral canthus (LC). In general, the BoNT are injected above and below this point along the orbital rim. Multipoint or multilevel injection techniques can be used to achieve a full zone of treatment, along with different injection methods according to the position of the eyebrows.[3,4,5] Meanwhile, injecting BoNT into the lateral and lower aspects of the OOc and the most lateral portion of the OOc is not recommended. While the former may weaken the zygomaticus major muscle (ZMj), resulting in an inability to elevate the corners of the mouth; the latter takes into consideration the possibility of anatomical variations of the OOc, which may weaken the lateral muscular band of the OOc and lead an asymmetrical unnatural smile.[2,6] The positional relationship between the OOc, zygomaticus minor (Zmi), and ZMj is the main consideration for determining the precise injection point.[2,7,8,9,10]

Although extensive injection guidelines on BoNT treatment have been reported, most treatments are administered by blind injection.[3,4,5] Furthermore, few studies have investigated the dynamic analyses of the formation of crow's feet, including detailed anatomical investigation of the orbital portion of the OOc via ultrasonography, to date. Moreover, previous research on the anatomical relationship between the OOc, Zmi, and ZMj has been done on fixed cadavers, and a majority of the individuals comprised aged donors. It is well known that the topography of the facial muscles in aged and young individuals is significantly different.

Ultrasonography has recently been used to examine the craniofacial area in order to target small muscles or determine precise injection points, as it can identify muscle and soft tissue layers in real time.[1,11,12,13] A previous study comparing conventional blind injection

and ultrasonography-guided BoNT injection found that ultrasonography-guided BoNT injection successfully increased the safety and reliability during the procedure. When using ultrasonography, clinicians can precisely confirm the target muscle and needle position to avoid complications.[14] Muscle movement and the detailed surrounding anatomy can also be monitored. Further, Sihler's staining can be used to represent the nerve density, distribution, and pathways in the facial area, thereby providing an effective guideline for BoNT injection.[15]

The aim of this study was to demonstrate the anatomical information of the OOc self, including muscle width, thickness, dynamic features and anatomical relationship between the OOc and the zygomaticus complex muscles using ultrasonography, as well as to visualize the distribution of the facial nerve that innervates the OOc using Sihler's staining, thereby providing reference data for BoNT injection targeting OOc.

2. Materials and Methods

2.1. Subjects and ultrasonography device

The 40 hemiface data were collected for ultrasonography from 20 healthy South Korean volunteers (7 men and 13 women; mean age, 28.9 years) with no history of facial cosmetic procedures in the past 6 months. And a total of 11 OOc specimens obtained from frozen cadavers of donors with no history of facial trauma or plastic surgery were included in this study. The study was conducted in accordance with the guidelines of the Declaration of Helsinki and was approved by the Institutional Review Board of the institution overseeing this research (IRB approval number: 2-2023-0050). The cadavers used in the present study were legally donated to institutes and subjected to dissection of the orbital region after receiving approval from the institution overseeing this research. The subjects had provided consent for donating their bodies for research purposes. The author state that every effort was made to follow all local and international ethical guidelines and laws that pertain to the use of human cadaveric donors in anatomical research.[16] The volunteers were placed in a semi-supine position for ultrasonography. The width, thickness, dynamic movement of the OOc and anatomical relationship between the OOc and zygomaticus complex muscles were measured and monitored using a real-time two-dimensional B-mode ultrasound device with a high-frequency (16 MHz) liner transducer (Sonimage HS1, KONICA MINOLTA, Tokyo, Japan)

2.2. Ultrasonography of crow's feet formation and the width and thickness of the OOc

Volunteers were asked to relax their faces, then smile while squinting their eyes hard. This caused the OOc to lift the labial commissure to maximize the visualization of the crow's feet to determine the movement of the OOc during the formation of the crow's feet and allowed the researchers to measure the width and thickness of the OOc. As shown in **Figure 1**, a horizontal line was drawn laterally from the LC, and landmarks were marked where this line intersected with the orbital rim (OR), the midpoint of the frontal process of zygomatic bone (M), and lateral margin of the frontal process of zygomatic bone (point B).

Point C refers to the 5 mm lateral to point B. Ultrasonographic examination was performed at this lateral canthus horizontal plane (LCHP) by placing the transducer on the outer orbit. The width of the OOc, the depth of the OOc from the skin surface (combining thickness of the skin and subcutaneous tissue), and the thickness of the OOc were measured using the ImageJ program (National Institutes of Health) (**Figure 2**). Descriptive statistics were used to describe the distribution of OOc. Independent t-test were performed to assess the differences between male and female volunteers and between the left and right-side measurements. The level of significance was set at $p < 0.05$.

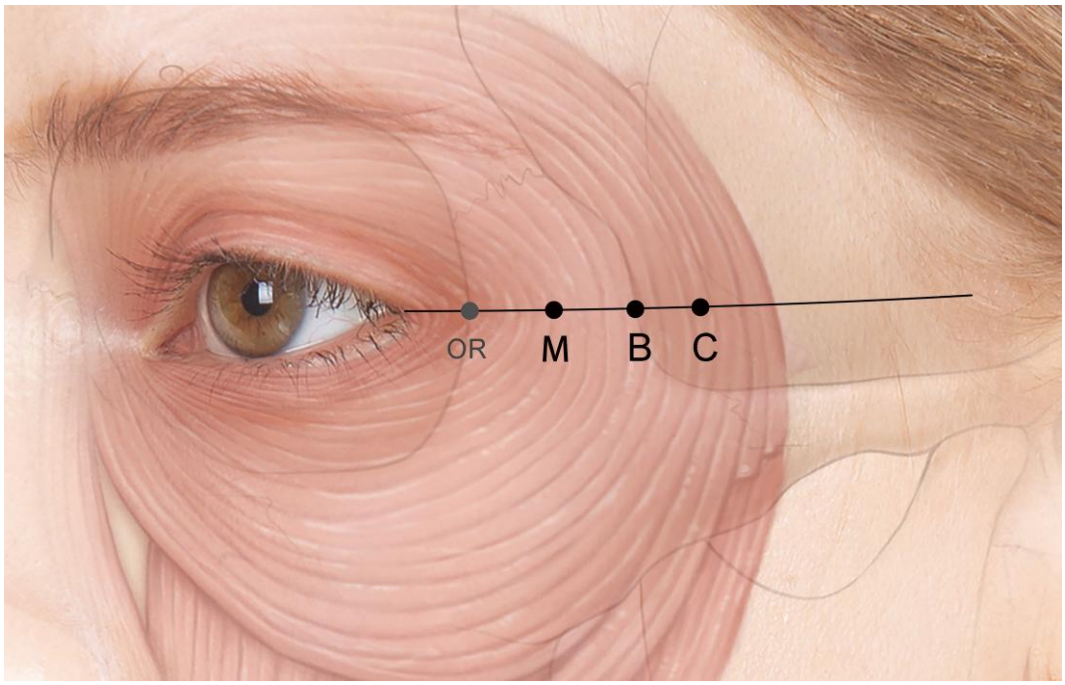

Figure 1. Surface landmark for measuring the width and thickness of the orbicularis oculi muscle.

A horizontal line was drawn laterally from the lateral canthus and landmarks were designated where this line intersected with the frontal process of zygomatic bone (OR, orbital rim; M, the midpoint of the frontal process of zygomatic bone; B, the point at the lateral margin of the frontal process of zygomatic bone; C, the point 5 mm lateral to point B at the lateral canthus level, respectively).

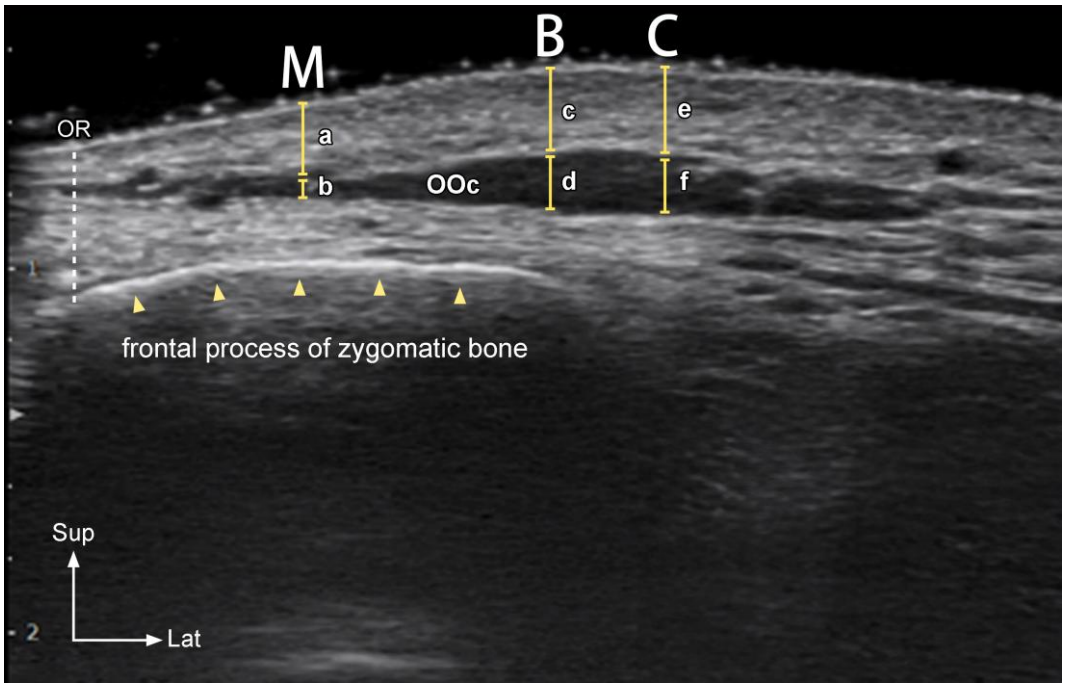

Figure 2. Ultrasonographic analysis of the orbicularis oculi muscle.

Each parameter was measured at three landmarks. OR, orbital rim; M, the midpoint of the frontal process of zygomatic bone; B, the point at the lateral margin of the frontal process of zygomatic bone; C, the point 5 mm lateral to point B at the lateral canthus level, respectively. (a), the depth of the OOc from the skin surface at point M; (b), the thickness of the OOc at point M; (c), the depth of the OOc at point B; (d), the thickness of the OOc at point B; (e), the depth of the OOc at point C; (f), the thickness of the OOc at point C.

2.3. Positional relationship between the OOc, Zmi, and ZMj

The positional relationship and overlapping ranges between the OOc, Zmi, and ZMj, as well as their distances from the skin, were measured on four different perpendicular reference lines. A horizontal line was drawn laterally from the LC and landmarks were marked where this line intersected with the LC, OR, and M point. The jugale point (J) was confirmed using the palpate method. The four perpendicular lines passing through the LC, OR, M, and J were established. Ultrasonographic examination was performed at these lines by aligning the edge of the transducer with the lateral canthus horizontal plane (LCHP) (**Figure 3**). In each perpendicular plane, the superficially located OOc and deeply located bony origins of the Zmi and ZMj can be identified (**Figure 4**). We measured 4 parameters on each reference line. The distance from the LCHP to the superior margin of the Zmi and ZMj, and to the inferior margin of the OOc was measured. The depth of these muscles was measured in the horizontal plane of the superior margin of the Zmi and ZMj (**Figure 5**). The positional relationship and overlapping ranges of the OOc, Zmi, and ZMj, in conjunction with the depth of these muscles, were measured using ImageJ program (National Institutes of Health, Bethesda, MD, USA).

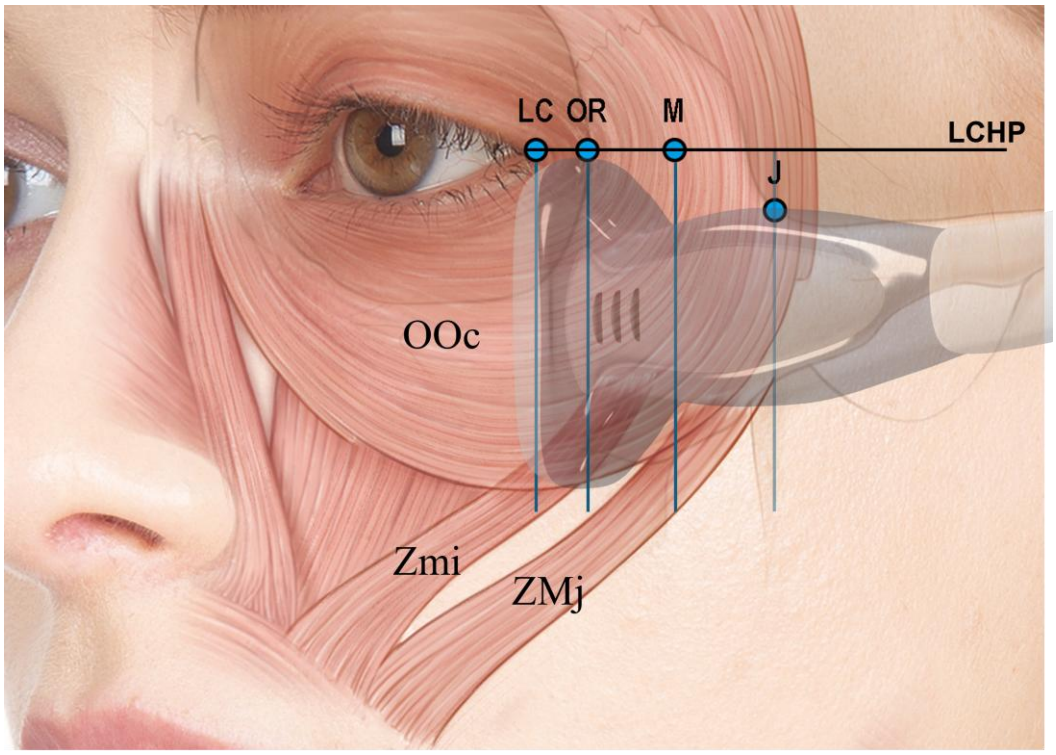

Figure 3. Illustration representing reference lines for ultrasonographic examination of the orbicularis oculi muscle and zygomaticus complex muscles.

A horizontal line was drawn laterally from the lateral canthus (LC), and the 3 landmarks were marked where this line intersected with the LC, OR and M point. The J referred to jugale point. There were 4 perpendicular lines passing through the LC, OR, M and J. OR, orbital rim; M, the midpoint of the frontal process of zygomatic bone; J, jugale point; OOc, orbicularis oculi muscle; Zmi, zygomaticus minor muscle; ZMj, zygomaticus major muscle; LCHP, lateral canthus horizontal plane.

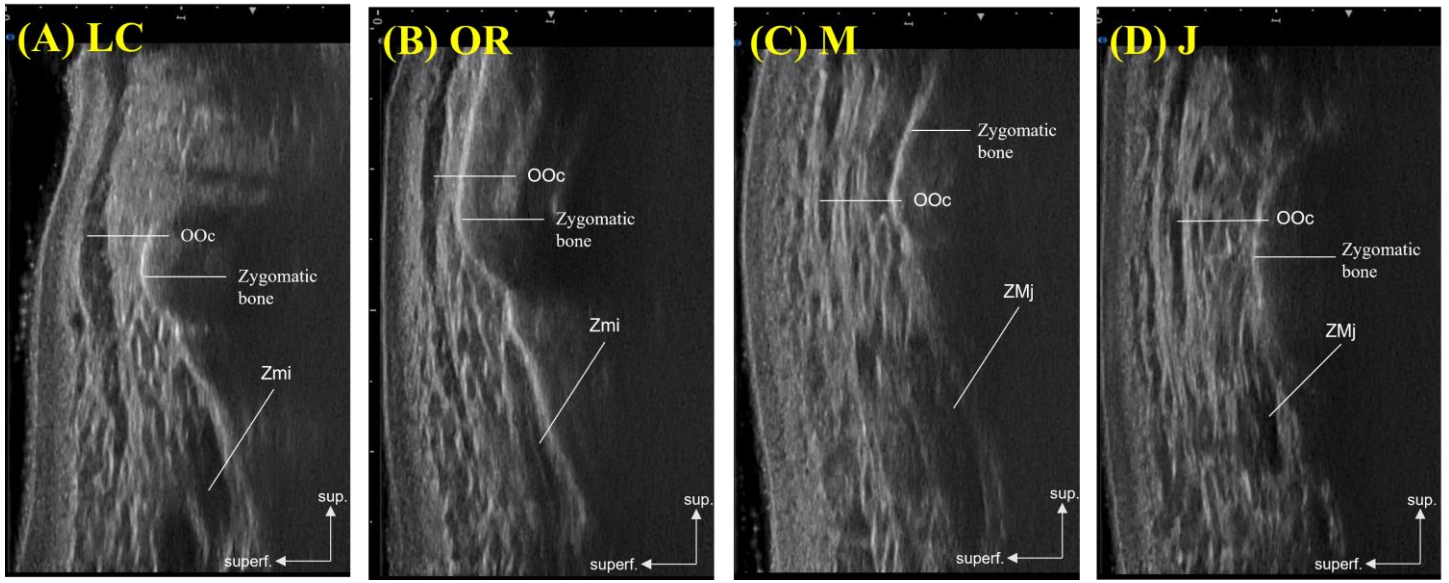

Figure 4. Ultrasonographic examination of the orbicularis oculi muscle and the zygomaticus complex muscles.

(A) B mode image of the OOc and zygomaticus minor muscle (Zmi) at the perpendicular plane LC. (B) B mode image of the OOc and Zmi at the perpendicular plane OR. (C) B mode image of the OOc and zygomaticus major muscle (ZMj) at the perpendicular plane M. (D) B mode image of the OOc and ZMj at the perpendicular plane J. LC, lateral canthus; OR, orbital rim; M, the midpoint of the frontal process of zygomatic bone; J, jugale point.

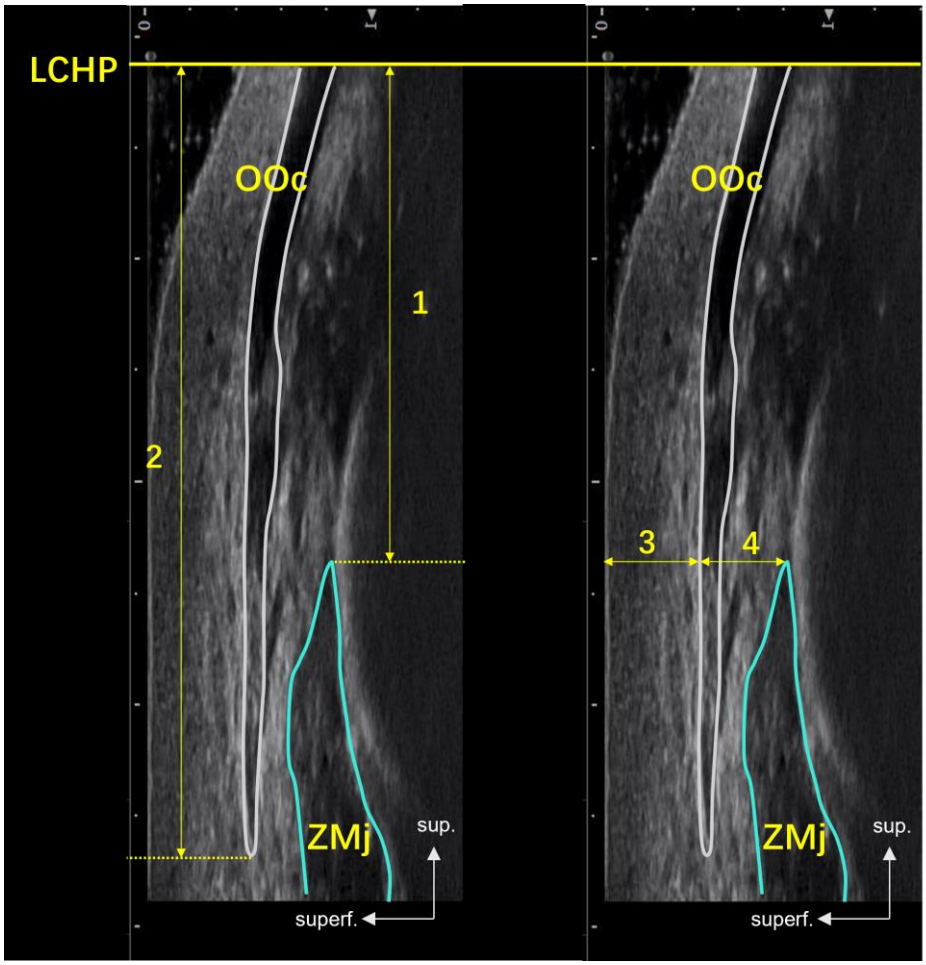

Figure 5. The 4 parameters measured on ultrasonographic examination of the orbicularis oculi muscle and the zygomaticus complex muscles.

1, the distance from the superior margin of the zygomaticus complex muscles to the lateral canthus horizontal plane (LCHP); 2, the distance from the inferior margin of the orbicularis oculi muscle (OOc) to the LCHP; 3, the distance from the epidermis to the surface of the OOc in the horizontal plane of the superior margin of the zygomaticus complex muscles; 4, the distance from the OOc to the surface of the zygomaticus complex muscles in the horizontal plane of the superior margin of the zygomaticus complex muscles. ZMj, zygomaticus major muscle.

2.4. Sihler's staining

Sihler's staining seriously impacts the morphology of the tissue, which may undergo significant shrinkage and distortion. Therefore, in order to accurately present the facial nerve topography on the stained specimens, we marked the bony landmark by tying knots prior to removing the specimen, ensuring easily identifiable and less anatomically variable landmark. Construction of a semicircular arc using the designated OR point as the center and the distance from the OR to the latera margin of the OOc at the LCHP as the radius ensured accuracy of nerve distribution representation after staining (**Figure 6**). These cadavers were meticulously dissected, and the OOc with neighboring soft tissues were isolated. Sihler's staining was implemented on each specimen as follows:

Fixation

The dissected specimens were fixed in a 10% unneutralized formalin for 14 days, with the solution being replaced when cloudy.

Maceration and depigmentation

The fixed specimens were washed under running tap water for 60 min. The specimens were placed in a 3% aqueous solution of potassium hydroxide with 0.2 mL of 3% hydrogen peroxide per 100 mL for 4 weeks; the solution was changed every day.

Decalcification

The macerated specimens were washed under running tap water for 60 min. They were placed in Sihler's solution I (1:1:6 of glacial acetic acid, glycerin, and 1% aqueous chloral hydrate) for 3 weeks; the solution was changed once a week.

Staining

The decalcified specimens were then colorized with Sihler's solution II (1:1:6 of Ehrlich hematoxylin, glycerin, and 1% aqueous chloral hydrate) for 3-4 weeks.

Destaining

The stained specimens were washed for 60 min and then placed in Sihler's solution I; the solution was changed whenever it turned purple. The process was terminated when the stained nerve fibers started to exhibit signs of fading.

Neutralization

The destained specimens were washed for 60 min and then placed in 0.05% lithium carbonate solution for 1 hour.

Cleaning

The specimens were placed in a series of increasing concentrations of glycerin (from 40% to 100%, with the concentration being increased by 20% every day).

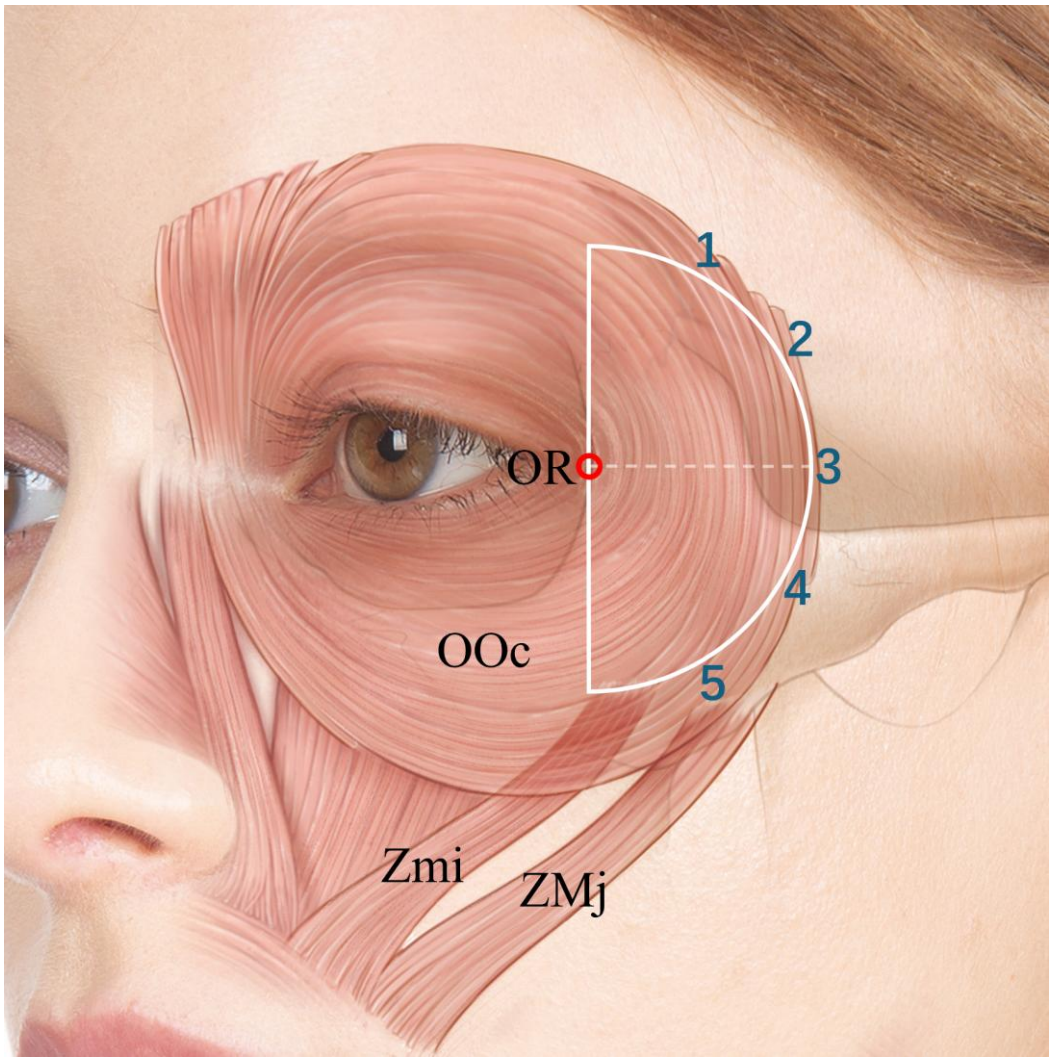

Figure 6. A schematic semicircular model of the orbicularis oculi muscle for Sihler's staining.

A schematic representation of the orbicularis oculi muscle (OOc) was delineated as a semicircular model using the orbital rim (OR) point as the center and the distance from the OR to the lateral margin of the OOc at the lateral canthus horizontal plane as the radius. Zmi, zygomaticus minor muscle; ZMj, zygomaticus major muscle.

3. Results

3.1. Ultrasonography of crow's feet formation and the width and thickness of the OOc

3.1.1 Contraction of the OOc during crow's feet formation

The OOc was shown as a hypoechoic image beneath the skin with irregular hyperechoic subcutaneous fat above the muscle during ultrasonography. Lateral movement of the transducer revealed that the OOc became thicker, and the lateral margin of the OOc was found at the superficial layer of the anterior temple (**Figure 7A**).

During the formation of dynamic crow's feet, the contraction of the orbital portion of the OOc moved the skin of the lateral orbital rim toward the LC, causing fine wrinkles in the thin skin (**Figure 7B**). Under ultrasonography in the horizontal view, it was also observed that the lateral portion of the OOc contracted during medial movement as the crow's feet formed. At the crow's feet formation stage, it was shown that the contracted orbital part of the OOc was thicker than that in the relaxed state. (**Figure 7A, B**).

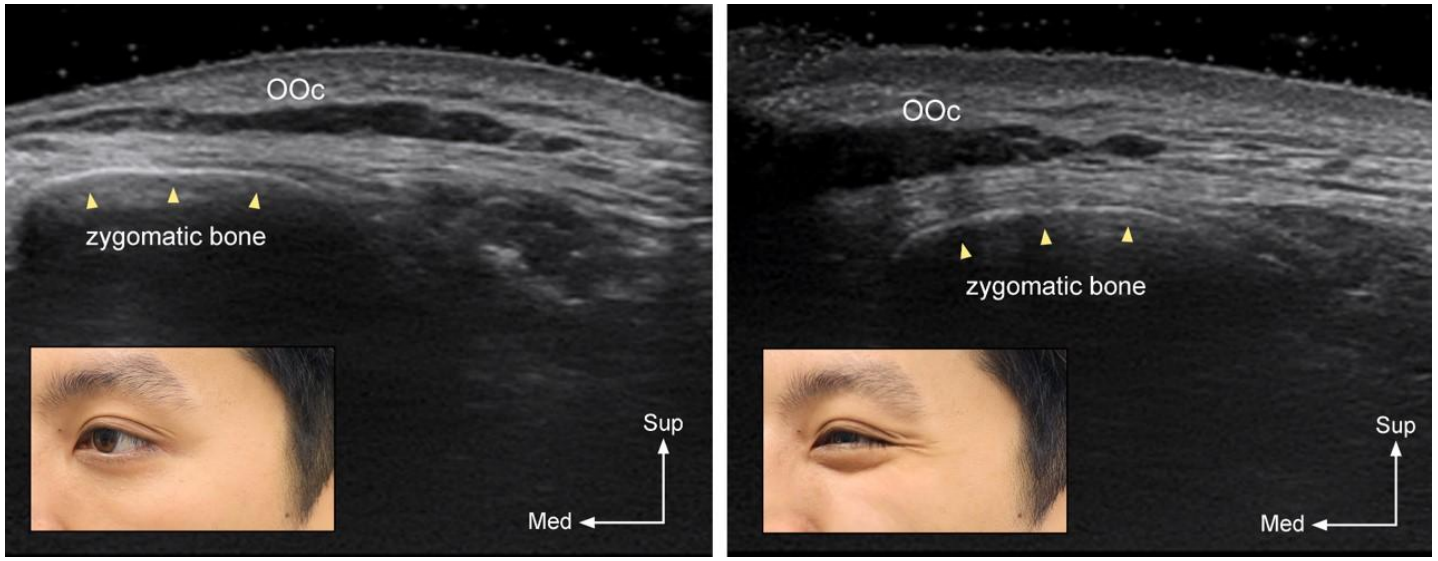

Figure 7. Dynamic ultrasonography performed during crow's feet formation.

Left and right ultrasound images were taken while the face was relaxed and when crow's feet formed, respectively. OOc, orbicularis oculi muscle.

3.1.2 Width and thickness of the OOc

At the LCHP, the mean length between the point B and the most lateral margin of the OOc was 12.5 ± 1.3 mm. These measurements did not differ significantly between the sexes and sides ($p > 0.05$). The depth of the OOc from the skin surface at points M, B, and C was 2.0 ± 0.4 mm, 2.8 ± 0.4 mm and 3.1 ± 0.5 mm, respectively. The depth of the OOc muscle differed between the sexes, and it was significantly greater in females compared to that of males ($p < 0.05$) (**Figure 8** and **Table 1**).

The muscle thicknesses of the OOc at points M, B, and C were 0.7 ± 0.3 mm, 1.1 ± 0.3 mm, and 1.2 ± 0.3 mm, respectively. No significant differences in muscle thickness measurements were found between the sexes and sides at most points except gender differences in muscle thickness at point C. The lateral portion of the OOc located lateral to point B was clearly demonstrated to be the thickest (**Figure 8** and **Table 1**).

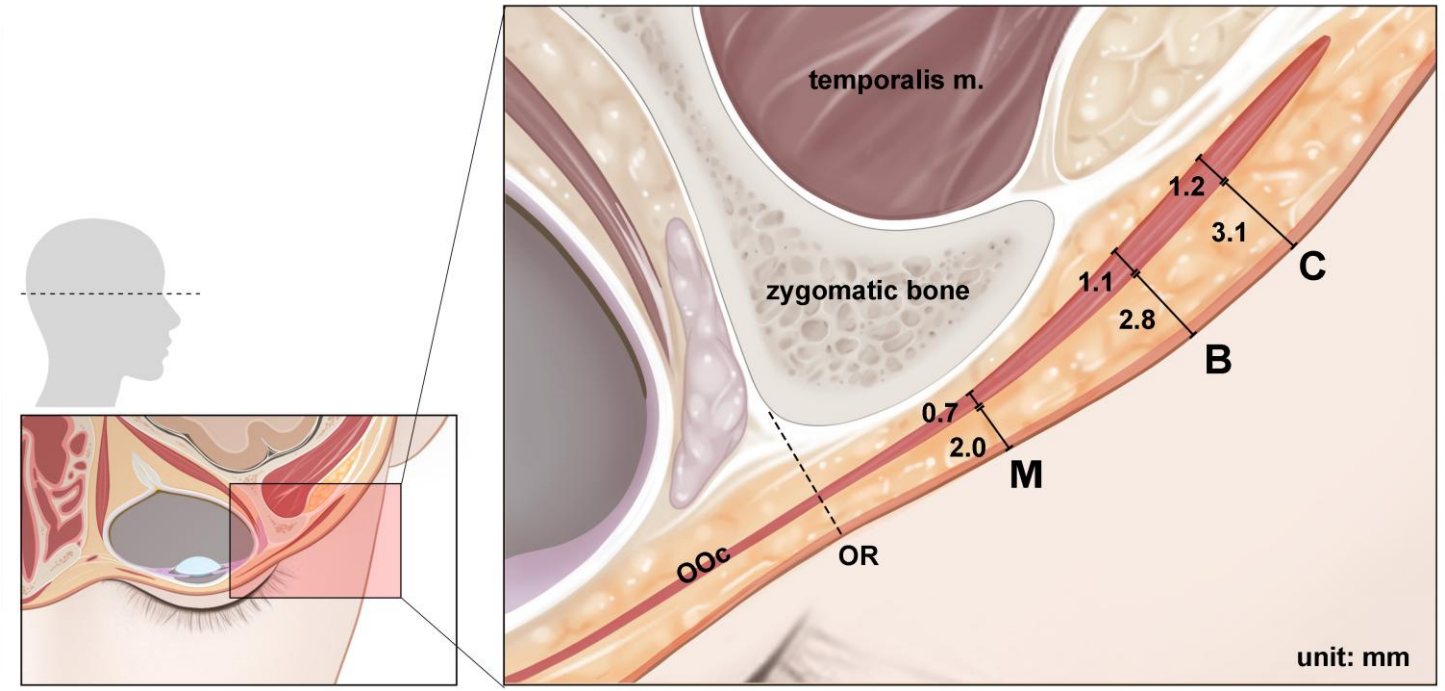

Figure 8. Mean depth and thickness of the orbicularis oculi muscle at lateral canthus horizontal plane.

OR, the point at the orbital rim; M, midpoint of the frontal process of zygomatic bone; B, the point on the lateral margin of the frontal process of zygomatic bone; C, the point 5 mm lateral to B at the lateral canthus horizontal plane; OOc, orbicularis oculi muscle.

Table 1. Mean depth and thickness of the orbicularis oculi muscle at lateral canthus horizontal plane.

Landmarks		Thickness	P-value	Depth	P-value
M	Male	0.7 ± 0.2	0.616	1.8 ± 0.4	0.001*
	Female	0.7 ± 0.3		2.2 ± 0.3	
B	Male	1.1 ± 0.3	0.311	2.6 ± 0.5	0.034*
	Female	1.0 ± 0.3		2.9 ± 0.3	
C	Male	1.4 ± 0.3	0.001[a]	2.9 ± 0.5	0.003*
	Female	1.1 ± 0.3		3.4 ± 0.5	

Note: Data are presented as mean ± SD values. Values are expressed in mm.

Abbreviation: SD, standard deviation; M, midpoint of the frontal process of zygomatic bone; B, the point on the lateral margin of the frontal process of zygomatic bone; C, the point 5 mm lateral to B at the lateral canthus horizontal plane.

*Statistically different between sexes ($p < 0.05$).

3.1.3 Determination of BoNT injection points for crow's feet

The movement of the OOc can be visualized and monitored using dynamic images of ultrasonography. The OOc contracted toward the lateral canthus and appeared to thicken during the formation of the crow's feet. Closer inspection of the dynamic ultrasound images showed that the thicker lateral portion of the OOc lateral to point B played a major role in the formation or crow's feet.

Therefore, based on our results, we propose a more effective novel BoNT injection guideline for improving the crow's feet. Compared to conventional injection guidelines, the novel BoNT injection included additional injection lateral to point B. We administered the injection intradermally into the relatively thin OOc portion (0.7 mm) with a relatively thinner subcutaneous layer (2.0 mm) that was not easy to target medial to point B under ultrasonographic guidance. Simultaneously, we administered the ultrasonography-guided intramuscular injection into the portion of the thicker OOc (1.2 mm) with an abundant subcutaneous layer (3.1 mm) lateral to point B (**Figure 9**).

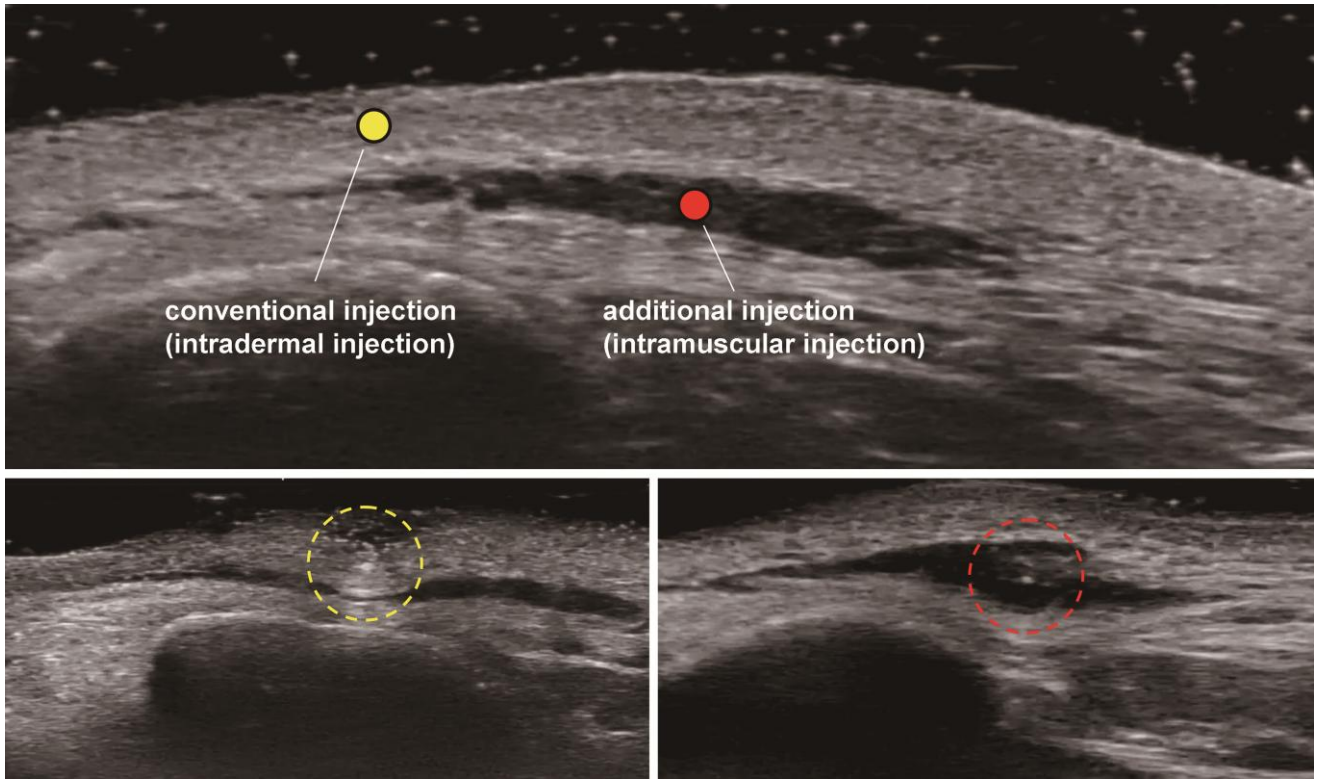

Figure 9. Ultrasonography demonstrating the novel BoNT injection guideline.

Yellow circle, intradermal injection; red circle, intramuscular injection; yellow and red dotted circles, needle tip visualized during ultrasound-guided injection.

3.2. Positional relationship between the OOc, Zmi, and ZMj

3.2.1 The location of the Zmi, ZMj superior margin and OOc inferior margin at each perpendicular plane

The distances of the Zmi, ZMj superior margin, and OOc inferior margin with reference to the LCHP at each perpendicular plane are presented in **Figure 10** and **Table 2**. The mean distances between the LCHP and the superior margin of the zygomaticus complex muscles were 20.0 mm (13.0-25.1 mm), 17.9 mm (10.2-26.9 mm), 22.8 mm (17.4-26.0 mm), and 20.8 mm (14.3-27.1 mm) at perpendicular plane LC, OR, M and J, respectively. The mean distances between the LCHP and OOc inferior margin were 23.8 mm (18.0-32.5 mm), 21.7 mm (16.3-29.2 mm), 21.3 mm (17.2-25.8 mm), and 20.1 mm (15.6-28.3 mm) at perpendicular plane LC, OR, M, and J respectively. While the locations of the Zmi and ZMj showed greater variability at the perpendicular plane OR than at the others, those of the OOc exhibited greater variability at the perpendicular plane LC than at the others. We found no statistically significant differences between the sexes, or between the left and right sides ($p > 0.05$).

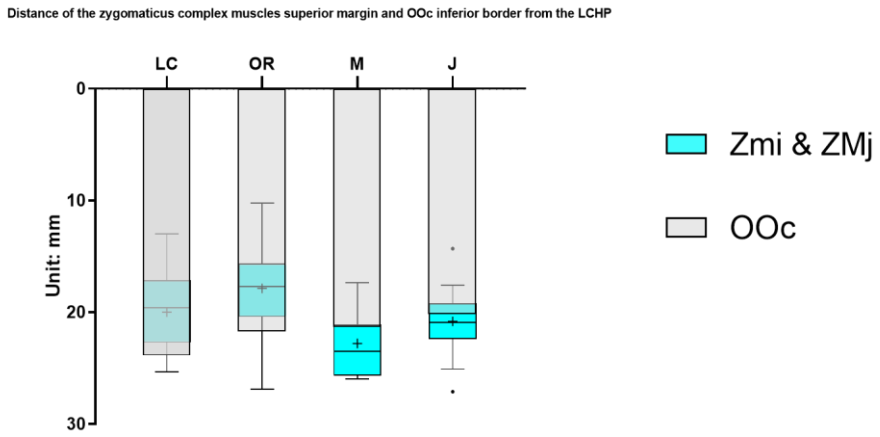

Figure 10. Distance of the zygomaticus complex muscles superior margin and orbicularis oculi muscle inferior margin from the lateral canthus horizontal plane.

LC-Box plot, the distance from the Zmi & ZMj superior margin to the lateral canthus horizontal plane (LCHP) at LC line. OR-Box plot, the distance from the Zmi & ZMj superior margin to the LCHP at OR line. M-Box plot, the distance from the Zmi & ZMj superior margin to the LCHP at M line. J-Box plot, the distance from the Zmi & ZMj superior margin to the LCHP at J line. LC-Bar chart, the distance from the OOc inferior margin to the LCHP at LC line. OR-Bar chart, the distance from the OOc inferior margin to the LCHP at OR line. M-Bar chart, the distance from the OOc inferior margin to the LCHP at M line. J-Bar chart, the distance from the OOc inferior margin to the LCHP at J line. LC, lateral canthus; OR, orbital rim; M, the midpoint of the frontal process of zygomatic bone; J, jugale point; OOc, orbicularis oculi muscle; Zmi, zygomaticus minor muscle; ZMj, zygomaticus major muscle.

Table 2. Distance of the zygomaticus complex muscles superior margin and orbicularis oculi muscle inferior margin from the lateral canthus horizontal plane.

	LC	OR	M	J
Zmi & ZMj				
Mean ± SD	20.0 ± 3.6	17.9 ± 3.9	22.8 ± 2.9	20.8 ± 2.7
Minimum	13.0	10.2	17.4	14.3
Maximum	25.1	26.9	26	27.1
OOc				
Mean ± SD	23.8 ± 4.1	21.7 ± 3.6	21.3 ± 2.8	20.1 ± 3.1
Minimum	18.0	16.3	17.2	15.6
Maximum	32.5	29.2	25.8	28.3

Note: N = 40, unit: mm.

Abbreviations: Zmi, zygomaticus minor muscle; ZMj, zygomaticus major muscle; OOc, orbicularis oculi muscle; LC, lateral canthus; OR, orbital rim; M, the midpoint of the frontal process of zygomatic bone; J, jugale point.

3.2.2 Depth of the Zmi, ZMj, and OOc at each perpendicular plane

We measured the depth from the skin to the OOc and from the OOc to the zygomaticus complex muscles in the horizontal plane of the superior margin of the zygomaticus complex muscles (**Figure 11** and **Table 3**). The mean distances between the OOc and the skin were 4.9 mm (3.2-6.4 mm), 4.8 mm (2.6-6.7 mm), 5.5 mm (3.4-7.8 mm), and 4.7 mm (2.9-6.4 mm) at perpendicular plane LC, OR, M, and J, respectively. The mean distances between the zygomaticus complex muscles and the OOc were 3.0 mm (1.5-4.4 mm), 3.1 mm (1.5-4.9 mm), 4.5 mm (3.1-5.3 mm), and 4.1 mm (2.5-6.4 mm) at perpendicular plane LC, OR, M, and J, respectively. We found no statistically significant differences between the sexes, or between the left and right sides ($p > 0.05$).

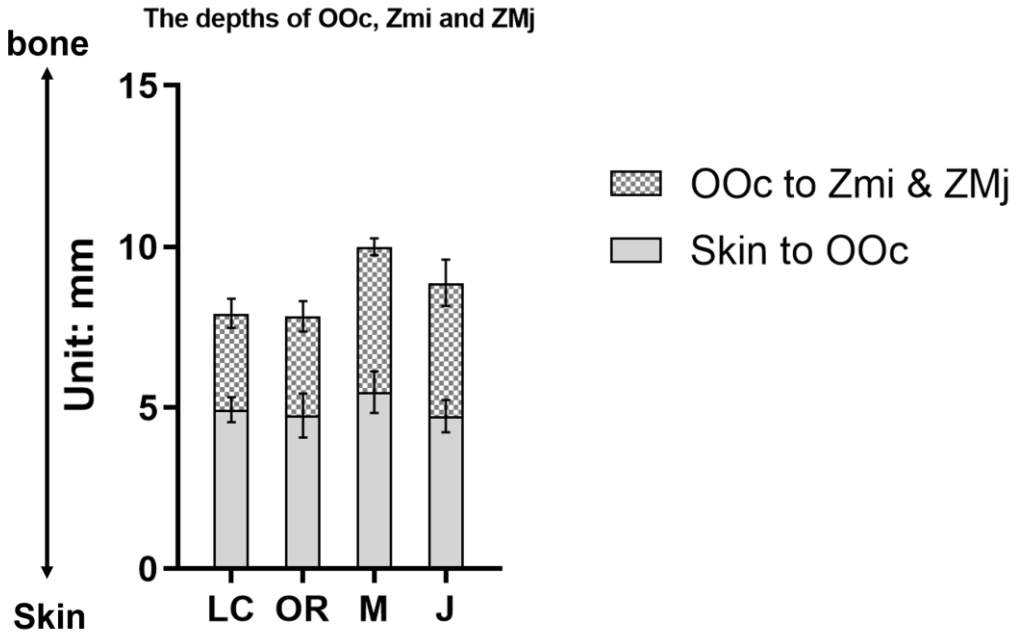

Figure 11. Depths of the orbicularis oculi muscle and the zygomaticus complex muscles in the horizontal plane of the superior margin of the zygomaticus complex muscles.

The gray diagram indicates the distance from the skin to the OOc includes the thickness of the skin, subcutaneous tissue. The dotted diagram indicates the distance from the OOc to the Zmi & ZMj. OOc; orbicularis oculi muscle; Zmi, zygomaticus minor muscle; ZMj: zygomaticus major muscle; LC, lateral canthus; OR, orbital rim; M, the midpoint of the frontal process of zygomatic bone; J, jugale point.

Table 3. Depths of the orbicularis oculi muscle and the zygomaticus complex muscles in the horizontal plane of the superior margin of the zygomaticus complex muscles.

	LC	OR	M	J
Skin to OOc				
Mean ± SD	4.9 ± 0.4	4.8 ± 0.7	5.5 ± 0.6	4.7 ± 0.5
Minimum	3.2	2.6	3.4	2.9
Maximum	6.4	6.7	7.8	6.4
OOc to Zmi & ZMj				
Mean ± SD	3.0 ± 0.5	3.1 ± 0.5	4.5 ± 0.3	4.1 ± 0.7
Minimum	1.5	1.5	3.1	2.5
Maximum	4.4	4.9	5.3	6.4

Note: N = 40, unit: mm.

Abbreviations: Zmi, zygomaticus minor muscle; ZMj, zygomaticus major muscle; OOc, orbicularis oculi muscle; LC, lateral canthus; OR, orbital rim; M, the midpoint of the frontal process of zygomatic bone; J, jugale point.

3.3. Sihler's staining

After staining procedure, semi-transparent OOc and transparent soft tissues were obtained. This facilitated the visualization of facial nerve distribution within the OOc and the nerve pathway in the soft tissues, discernible up to the fine terminals with the naked eyes.

The nerve branches laterally converging toward the muscle tissue were densely distributed in the 1-4 o'clock range of the semicircular model (**Figure 12**). It is evident from the diagram that this region is appropriate for injection, and that the zygomaticofacial nerve located below the 4 o'clock range must be avoided. The nerve distribution revealed by Sihler's staining appears consistent with that seen in previous gross anatomical investigations.[15,17] However, we found during stereomicroscopy (Leica MZ FLIII, Heerbrugg, Switzerland; 10× magnification) that the facial nerve does not travel within the OOc, but through the soft tissue beneath it. Stereomicroscopy showed that distribution of the facial nerve does not follow a pattern where some nerves terminate at the orbital part and others terminate at the palpebral part. Instead, the facial nerve fibers continuously travel through the orbital part without termination. As the facial nerve progresses, it branches out into fine branches to innervate the orbital part of the OOc, which is located superficially (**Figure 13**).

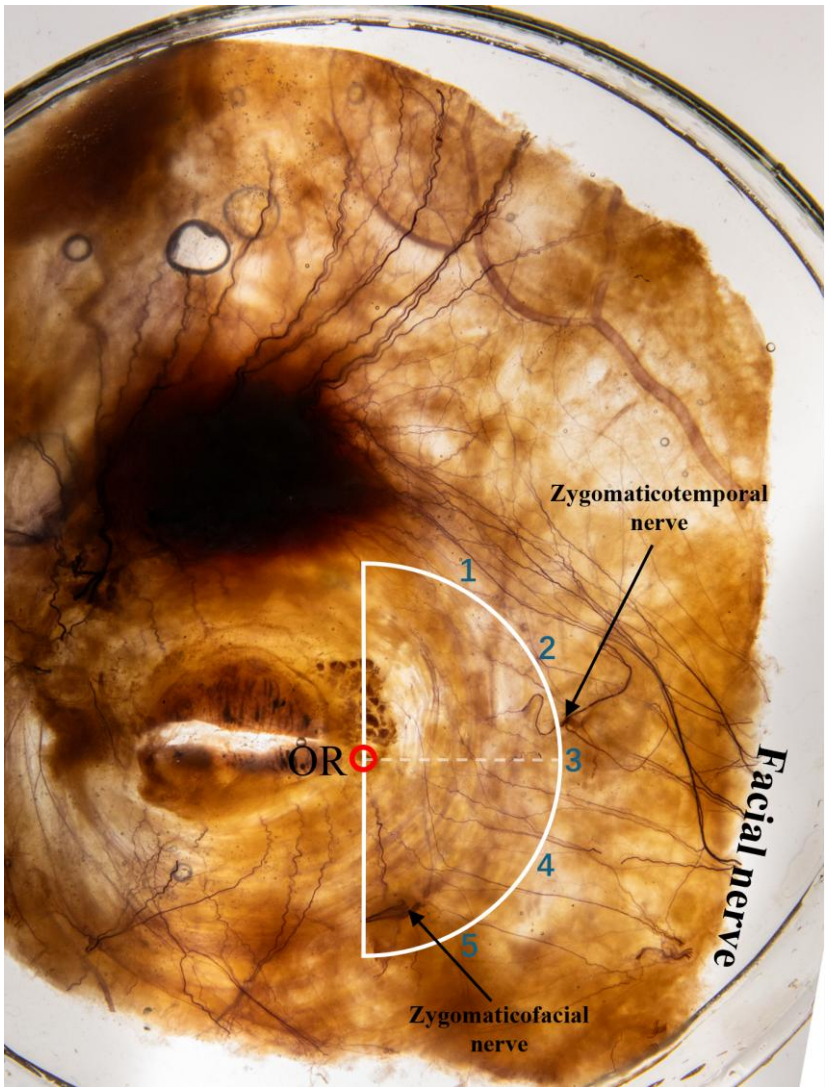

Figure 12. Facial nerve distribution within the orbicularis oculi muscle.

OR, the point at the orbital rim.

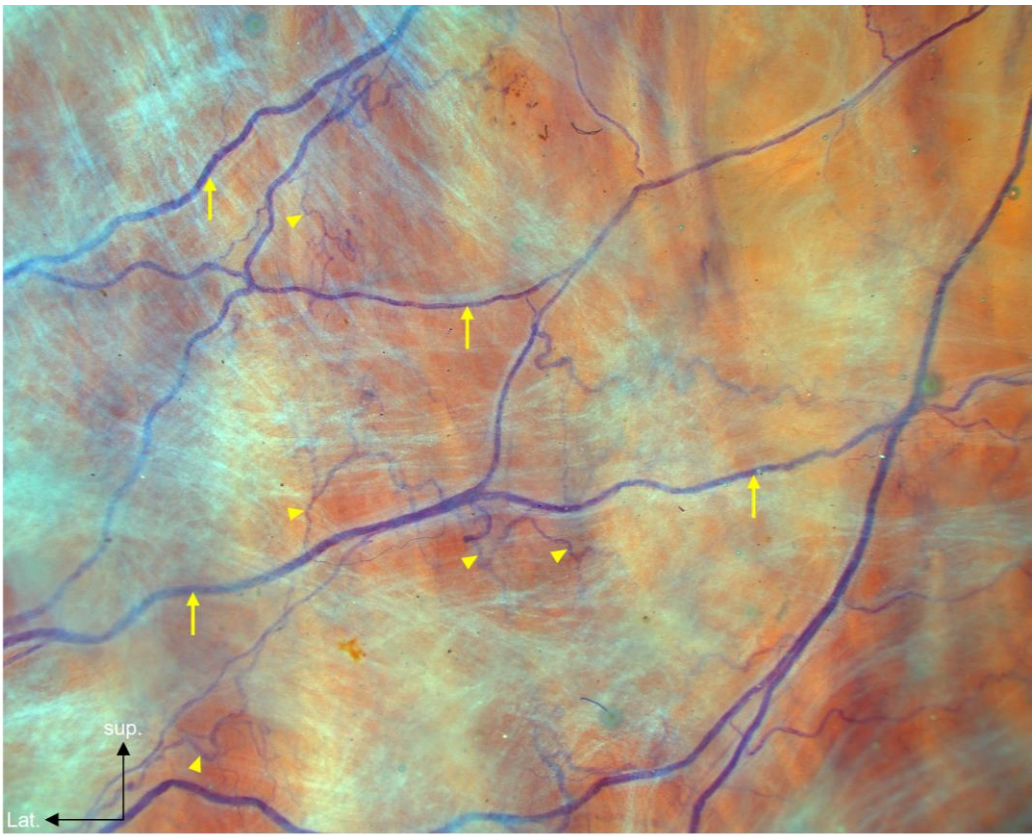

Figure 13. Posterior view of the orbicularis oculi muscle with Sihler's staining.

This image corresponds to the enlarged OOc at 10× magnification. The facial nerve (arrow, purple staining) travels beneath OOc and branches out into fine branches (arrowhead) to innervate the OOc located superficially.

4. Discussion

Two major etiologic factors of wrinkle formation have been proposed in the literature, namely the skin and facial expression muscles, and an effective treatment is paralysis of the facial muscles.[18] To reduce the obvious appearance of wrinkles, various esthetic treatments such as laser, high-intensity focused ultrasound, filler, and BoNT treatments have been developed for patients to choose from.[19] Among them, BoNT is one of the representative treatments targeting muscles and has been used extensively to treat crow's feet.[20] BoNT for facial wrinkles is the most frequently performed and popular cosmetic procedure approved by the Food and Drug Administration, with few side effect, significant effect, and good patient satisfaction.[21,22,23]

Although extensive injection guidelines on crow's feet have been provided, no studies on the anatomical analyses of the OOc exist to our knowledge. And some associated complications have been reported. As the toxin infiltrates not only the targeted OOc but also the adjacent Zmi and ZMj, patients may exhibit symptoms of Bell's palsy.[24,25] This emphasizes the need for precise targeting of the injection. If clinicians inadvertently inject the toxin into the overlapping Zmi or ZMj, patients may experience muscle weakness, resulting in an inability to elevate the corners of the mouth and upper lip. Understanding these anatomical relationships is paramount to avoiding the risk of adverse complications. This study aimed to propose anatomical evidence to facilitate precise crow's feet treatment by elucidating the anatomical information of the OOc self and positional relationship between the OOc and zygomaticus complex muscles, as well as the distribution of facial nerve visualization within the OOc musculature.

The previous study reported cases of intraoperative injection of BoNT into the OOc as a treatment for crow's feet. Intraoperative injection permits exact injection of the toxin due to direct vision and results in improvement in the crow's feet. The same effect can be obtained through precise targeted injection with noninvasive ultrasound-guided injections.[18] The establishment of various injection guidelines has resulted in intramuscular injection no longer being the only injection method for BoNT administration. The level of injection determines the potency of BoNT into the muscle; intramuscular injection has a strong effect, whereas intradermal injection has a soft effect.[4,26] Consequently, we combined the intradermal injection and intramuscular injection into the OOc. The fine wrinkles near the lateral canthus can be eliminated by intradermal injection. The

intramuscular injections could help in improving the deep furrows at the outer orbit during the dynamic contraction of the OOc.

In this study, we evaluated the positional relationship between the OOc and zygomaticus complex muscles based on 4 different perpendicular planes. In contrast to previous studies, we determined the overlapping ranges and depth of the OOc and the zygomatic complex muscles using ultrasonographic examination in young individuals and performed Sihler's staining of fresh cadavers. Our study provides clinical anatomic information that can help practitioners target the BoNT injection more precisely. We investigated bony origins of the Zmi and ZMj along each perpendicular plane based on sagittal ultrasound images of the lateral part of the OOc. Considering the average distance between the superior margin of the Zmi and ZMj and the inferior margin of the OOc from the LCHP on the four perpendicular planes can allow us to avoid injections into the overlapping region. The ultrasound images make it evident that the thickness of the subcutaneous tissue gradually increases from the superior to the inferior aspect, indicating an increase in muscle depth. This is consistent with those of a previous study that used a three-dimensional scanning system to determine the thickness of the facial skin and subcutaneous tissue.[27] Thus, we measured the muscle depth in the horizontal plane at the superior margin of Zmi or ZMj. Using this depth as a reference makes it feasible to avoid injections into the Zmi and ZMj even in the overlapping region.

We aimed to minimize the risk of OOc injection for crow's feet treatment by avoiding the lip elevator and mouth corner elevator muscles. Given the muscle overlapping, it is crucial not only to avoid injecting in the overlapping regions, but also to carefully consider the depth of the injection. Ultrasonographic visualization aids in determining the optimal injection method and dosage by providing precise insights into the location and layer of the target muscle.[28] Moreover, its non-invasive and nonradiative in nature and its ability to visualize anatomical variation enables assessment of facial muscle topography in young living subjects. The anatomical information acquired from young individuals is more appropriate for clinical applications than that acquired from fixed cadavers.

One limitation of this study is that the Zmi and ZMj we investigated were of bony origin, whereas in reality, the Zmi and ZMj consist of fibers originating from both bone and the OOc. Hur et al. reported that OOc fibers were involved in the composition of the Zmi in all specimens.[9] Kampan et al. reported that the lateral bundles of the OOc joined with the ZMj in all specimens, and with the Zmi in 63.6% of the 12 Japanese cadavers of Japanese individuals.[10] Another recent study suggests that the connection between the OOc and ZMj occurs in only 22.7%.[29] In contrast to typical skeletal muscle mass, the facial

expression muscles lack a distinct fascial envelope, and their thin and flat nature make it challenging to identify merged muscles in ultrasound images. Therefore, ultrasonography is unable to differentiate between muscle bundles originating from the zygomatic bone and those extending from the OOc. The origin of the Zmi and ZMj demonstrates variation across different ethnic groups. Data obtained from studies on African, Hawaiian, and Chinese populations indicate that the OOc are commonly connected to the undifferentiated zygomaticus muscle groups. Conversely in a majority of White subjects, the zygomaticus musculature is independent of the OOc, with no connection between them. Both of the Zmi and ZMj originate from the zygomatic arch.[30] Given that some of the fibers originate from the OOc, OOc toxin injection anatomically affects the zygomaticus complex muscles, which would affect upper lip and mouth corner movements. Nonetheless, this anatomical relationship has been explored in several studies recently. A previous study demonstrated that the anatomically variant lateral muscular band of OOc terminates at the corner of the mouth, and assessed the position of this band at the level of the LC.[2] Hur et al. suggested that the mean (± SD) width of the lateral fibers of the OOc that extended to the upper lip at the LC level was 6.9 (± 3.3 mm).[31] These data provide guidance on avoiding injecting into the OOc fibers that extend to the zygomaticus complex muscles. A previous study proposed that the formation of lower crow's feet and lateral cheek rhytides referred to accordion wrinkles, was attributed to the simultaneous contraction of the OOc and ZMj.[32] Thus, although anatomical information indicates that injecting into the connecting fibers of the OOc may affect the ZMj, such injection may assist in reducing accordion wrinkles. Further investigation is necessary to re-evaluate the effects of such injection on facial wrinkles and the balance of action.

Visualization of the nerve on the orbital region can improve understanding of the injection guidelines for crow's feet. Clinical, pharmacological, and anatomical factors are critical determinants of the efficacy and safety of BoNT injections. The technical approach to achieving effective injection is concerned with the efficiency of the agents that approach the intramuscular motor end plates.[33] Therefore, determining the nerve density within the targeted anatomical region is critical in ensuring optimal efficacy of BoNT administration.[34,35,36] Several studies have used conventional gross anatomical methods and revealed similar nerve distribution in the OOc as that reported in this study.[37,38] As Sihler's staining delineates nerve distribution with enhanced detail, it should be taken into consideration for BoNT injection. The BoNT injection guidelines about typical skeletal musculature have substantiated that the optimal injection points of the BoNT can be determined based on the abundance of neuromuscular junctions.[39] A previous study used microdissection and Sihler's staining to determine the arborization of the masseteric nerve

branches within the masseter muscle and proposed that injecting in the area with richest arborization facilitates the treatment of masseteric hypertrophy.[40] As the BoNT acts on nerve endings, anatomical knowledge about the location of the nerve endings on the target muscle is crucial for optimal efficacy with minimum BoNT dosage.[41] Nevertheless, unlike the masseteric nerve branching off twigs within the masseter muscle and innervating its superficial, middle, and deep layers, stereomicroscopy has shown a distinct pattern for the facial nerve on the OOc.

Stereomicroscopic magnification helps three-dimensional visualization of specimens, thereby allowing a thorough examination. It has shown that the facial nerve does not enter directly into the flattened OOc to branch off twigs, instead, it branches off to the OOc superficially as it progresses medially through the soft tissue beneath the OOc. Another study using histological staining of coronal sections along the reference line perpendicular to the jugale point revealed the facial nerve in the perpendicular plane, located within the soft tissue layer deep to the OOc.[13] Hence, the limitation of Sihler's staining lies in its difficulty to recommend precise injection points based on the richest distribution of nerve endings in the OOc, as the nerve distribution seen in this study is shown as the pathway of the facial nerve beneath the OOc. Instead, we recommend injection points based on the areas where nerve pathways were relatively concentrated in the stained specimen.

5. Conclusion

In this study, we proposed new insights for crow's feet injection based on anatomical information obtained from ultrasonography and Sihler's staining. Ultrasonography was used to quantify the width and thickness of the OOc, and the distances between the superior margin of zygomaticus complex muscles and the inferior margin of the OOc from the LCHP. In clinical practice, it is important that ultrasonographic examination reveals the anatomical variations among individuals in real time. Therefore, the results of this study would contribute to minimizing complications during the administration of BoNT for treating crow's feet.

References

1. Kim HJ, Youn KH, Kim JS, Kim YS, Hong SO. *Ultrasonographic Anatomy of the Face and Neck for Minimally Invasive Procedures: An Anatomic Guideline for Ultrasonographic-Guided Procedures*. Springer; 2021:103-125.

2. Park JT, Youn KH, Hur MS, Hu KS, Kim HJ. Malaris Muscle, the Lateral Muscular Band of Orbicularis Oculi Muscle. *Journal of Craniofacial Surgery*. 2011;22(2):659-662.

3. Kim HJ, Seo KK, Lee HK, Kim J. Clinical anatomy for botulinum toxin injection. In: Kim HJ, Seo KK, Lee HK, Kim J, eds. *Clinical Anatomy of the Face for Filler and Botulinum Toxin Injection*. Singapore: Springer; 2016:58-60.

4. Iozzo I, Tengattini V, Antonucci VA. Multipoint and multilevel injection technique of botulinum toxin A in facial aesthetics. *J Cosmet Dermatol*. 2014;13(2):135-142.

5. De Maio M, Swift A, Signorini M, Fagien S. Facial assessment and injection guide for botulinum toxin and injectable hyaluronic acid fillers: focus on the upper face. *Plast Reconstr Surg*. 2017;140(2):265e-76e.

6. Seo KK. *Botulinum Toxin for Asians*. Springer Singapore: Imprint: Springer; 2017:29-99.

7. Youn KH, Park JT, Park DS, Koh KS, Kim HJ, Paik DJ. Morphology of the Zygomaticus Minor and Its Relationship with the Orbicularis Oculi Muscle. *Journal of Craniofacial Surgery*. 2012;23(2):546-548.

8. Choi DY, Hur MS, Youn KH, Kim J, Kim HJ, Kim SS. Clinical anatomic considerations of the zygomaticus minor muscle based on the morphology and insertion pattern. *Dermatologic Surgery: Official Publication for American Society for Dermatologic Surgery [et Al]*. 2014;40(8):858-863.

9. Hur MS, Youn KH, Kim HJ. New Insight Regarding the Zygomaticus Minor as Related to Cosmetic Facial Injections. *Clinical Anatomy*. 2018;31(7):974-980.

10. Natnicha K, Tsutsumi M, Okuda I, et al. The malaris muscle: its morphological significance for sustaining the intraorbital structures. *Anatomical Science International*. 2017;93(3):364-371.

11. Bae H, Kim J, Seo KK, Hu KS, Kim ST, Kim HJ. Comparison between Conventional Blind Injections and Ultrasound-Guided Injections of Botulinum Toxin Type A into the Masseter: A Clinical Trial. *Toxins*. 2020;12(9):588.

12. Ahn HS, Kim JS, Lee HJ, Lee JH, Kim HM, Kim HJ. Anatomical Continuation Between the Sub-Superficial Musculoaponeurotic System Fat and Retro-Orbicularis Oculi Fat: The True Nature of the Retro-Orbicularis Oculi Fat. *Facial Plastic Surgery & Aesthetic Medicine*. 2020;23(5).

13. Lee HJ, Kim HM, Ahn HS, Lee JH, Kim HJ. Novel Clinical Anatomic Consideration of the Superficial and Deep Layers of the Deep Temporal Fascia. *Plastic & Reconstructive Surgery*. 2023;153(3).

14. Bae H, Kim J, Seo KK, Hu KS, Kim ST, Kim HJ. Comparison between conventional blind injections and ultrasound-guided injections of botulinum toxin type A into the masseter: A clinical trial. *Toxins (Basel)*. 2020;12(9):588.

15. Yang HM, Won SY, Kim HJ, Hu KS. Sihler staining study of anastomosis between the facial and trigeminal nerves in the ocular area and its clinical implications. *Muscle & Nerve*. 2013;48(4):545-550.

16. Iwanaga J, Singh V, Takeda S, et al. Standardized statement for the ethical use of human cadaveric tissues in anatomy research papers: Recommendations from Anatomical Journal Editors-in-Chief. *Clin Anat*. 2022;35(4):526-528.

17. Choi Y, Kim IB. Distribution of the Laterally Supplying Facial Nerve to the Orbicularis Oculi Muscle. *Aesthetic Surgery Journal*. 2020;41(2):161-169.

18. Guerrissi JO. Intraoperative injection of botulinum toxin A into orbicularis oculi

muscle for the treatment of crow's feet. *Plast Reconstr Surg.* 2000;105(6):2219-2225.

19. Keen M, Blitzer A, Aviv J, Binder W, Prystowsky J, Smith H, Brin M. Botulinum toxin A for hyperkinetic facial lines: results of a double-blind, placebo-controlled study. *Plast Reconstr Surg*. 1994;94(1):94-99.

20. Breidenbach MA, Brunger AT. New insights into clostridial neurotoxin–SNARE interactions. *Trends Mol Med.* 2005;11(8):377-381.

21. Sundaram H, Signorini M, Liew S, de Almeida AR, Wu Y, Braz AV, Fagien S, Goodman GJ, Monheit G, Raspaldo H. Global Aesthetics Consensus Group. Global aesthetics consensus: botulinum toxin type A—evidence-based review, emerging concepts, and consensus recommendations for aesthetic use, including updates on complications. *Plast Reconstr Surg.* 2016;137(2):518e-529e.

22. Small R. Botulinum toxin injection for facial wrinkles. *Am Fam Physician.* 2014;90(3):168-175.

23. Hexsel C, Hexsel D, Porto MD, Schilling J, Siega C. Botulinum toxin type A for aging face and aesthetic uses. *Dermatol Ther.* 2011;24(1):54-61.

24. Matilde M, Spósito M. New Indications for Botulinum Toxin Type A in Cosmetics: Mouth and Neck. *Plastic and Reconstructive Surgery*. 2002;110(2):601-611.

25. Spiegel JH, DeRosa J. The Anatomical Relationship between the Orbicularis Oculi Muscle and the Levator Labii Superioris and Zygomaticus Muscle Complexes. *Plastic and Reconstructive Surgery*. 2005;116(7):1937-1942.

26. Vachiramon V, Subpayasarn U, Triyangkulsri K, Jurairattanaporn N, Rattananukrom T. Different injection patterns of incobotulinumtoxinA for crow's feet: a split-face comparative study. *J Eur Acad Dermatol Venereol.* 2021;35(1):256-262.

27. Kim Y, Lee K, Kim J, et al. Regional thickness of facial skin and superficial fat: Application to the minimally invasive procedures. *Clinical Anatomy*.

2019;32(8):1008-1018.

28. Lee H, Kim JS, Youn KH, Lee J, Kim HJ. Ultrasound-Guided Botulinum Neurotoxin Type A Injection for Correcting Asymmetrical Smiles. *Aesthetic Surgery Journal*. 2018;38(9):NP130-NP134.

29. Iwanaga J, Hur MS, Kikuta S, Ibaragi S, Watanabe K, Tubbs RS. Anatomical contribution of the orbicularis oculi to the zygomaticus major: An improved understanding of the smile with consideration for facial cosmetic procedures. Zhou J, ed. *PLOS ONE*. 2022;17(7):e0272060.

30. Ernst H. Evolution of Facial Musculature and Facial Expression. *Journal of the American Medical Association*. 1932;98(12):1024.

31. Hur MS, Iwanaga J, Tubbs RS, Moon YS, Kim H. Width of the orbicularis oculi fibers extending to the upper lip with the lateral and inferior lengths of the orbicularis oculi at the lateral canthus level: application to botulinum neurotoxin type A injection for crow's feet. *Surgical and Radiologic Anatomy*. 2023;45(4):461-468.

32. Mole B. Accordion Wrinkle Treatment Through the Targeted Use of Botulinum Toxin Injections. *Aesthetic Plastic Surgery*. 2013;38(2):419-428.

33. Cho TH, Hong JE, Yang HM. Neuromuscular compartmentation of the subscapularis muscle and its clinical implication for botulinum neurotoxin injection. *Scientific Reports*. 2023;13(1).

34. Warden JM, Roberts SL, Chang Y, et al. Neuromuscular Partitioning of Subscapularis Based on Intramuscular Nerve Distribution Patterns: Implications for Botulinum Toxin Injections. *Archives of Physical Medicine and Rehabilitation*. 2014;95(7):1408-1415.

35. Li Y, Wang M, Tang S, Zhu X, Yang S. Localization of nerve entry points and the center of intramuscular nerve-dense regions in the adult pectoralis major and pectoralis minor and its significance in blocking muscle spasticity. *Journal of Anatomy*. 2021;239(5):1123-1133.

36. Wang J, Li Y, Wang M, Yang S. Localization of the Center of the Intramuscular Nerve Dense Region of the Suboccipital Muscles: An Anatomical Study. *Frontiers in Neurology*. 2022;13.

37. RAMIREZ O, SANTAMARINA R. Spatial orientation of motor innervation to the lower orbicularis oculi muscle. *Aesthetic Surgery Journal*. 2000;20(2):107-113.

38. Hwang K, Cho HJ, Chung IH. Pattern of the Temporal Branch of the Facial Nerve in the Upper Orbicularis Oculi Muscle. *Journal of Craniofacial Surgery*. 2004;15(3):373-376.

39. Lee HJ, Lee JH, Yi KH, Kim HJ. Intramuscular Innervation of the Supraspinatus Muscle Assessed Using Sihler's Staining: Potential Application in Myofascial Pain Syndrome. *Toxins*. 2022;14(5):310.

40. Kim DH, Hong HS, Won SY, et al. Intramuscular Nerve Distribution of the Masseter Muscle as a Basis for Botulinum Toxin Injection. *Journal of Craniofacial Surgery*. 2010;21(2):588-591.

41. Lee KL, Cho HJ, Bae H, Park HJ, Park MS, Kim HJ. Anatomical Considerations When Treating Compensatory Hypertrophy of the Upper Part of the Masseter after Long-Term Botulinum Neurotoxin Type A Injections. *Toxins*. 2020;12(3):202.

Abstract in Korean

초음파와 Sihler 염색 활용한 눈둘레근의 해부학적 고찰 및 주사법

눈둘레근은 타원형으로 넓고 편평한 근육으로, 수축 시 눈가주름을 형성하여 안면 노화와 밀접하게 연관된다. 보툴리눔독소는 눈둘레근를 표적으로 하는 대표적인 치료법 중 하나이다. 본 연구는 초음파를 이용하여 눈둘레근 자체의 해부학적 정보(근육의 폭, 두께, 움직임)와 눈둘레근, 큰광대근, 작은광대근 간의 해부학적 관계를 규명한다. 이와 더불어 Sihler 염색법을 활용하여 눈둘레근를 지배하는 얼굴신경의 분포를 시각화하여 눈둘레근를 표적으로 하는 보톨리눔독소 주사 자입점에 참고할 수 있는 데이터를 제공하는 것을 목적으로 한다.

본 연구는 한국인 20 명을 대상으로 임상 연구를 진행하여 데이터를 수집하였다. 눈둘레근의 폭, 두께, 움직임은 초음파를 사용하여 수평면에서 측정되었다. 눈둘레근과 작은광대근, 큰광대근 간의 위치 관계와 중첩되는 범위, 그리고 표피와의 거리는 네 개의 서로 다른 수직면에서 초음파를 통해 측정되었다. 마지막으로 Sihler 염색법으로 눈둘레근에 분포한 얼굴신경을 확인하였다.

가쪽눈구석 수평면에서 광대뼈이마돌의 가쪽 경계와 눈둘레근의 가장 가쪽 경계 간의 거리는 12.5 ± 1.3 mm 로 측정되었다. 광대뼈이마돌기 중점, 광대뼈이마돌기 가쪽 경계, 그리고 광대뼈이마돌기로부터 5 mm 가쪽 지점에서의 눈둘레근 깊이는

각각 2.0 ± 0.4 mm, 2.8 ± 0.4 mm, 3.1 ± 0.5 mm 로 측정되었다. 동일한 지점에서 눈둘레근 두께는 각각 0.7 ± 0.3 mm, 1.1 ± 0.3 mm, 1.2 ± 0.3 mm 로 측정되었다.

가쪽눈구석, 눈확가쪽모서리, 광대뼈이마돌기 중점, 그리고 광대뼈각점 지나는 수직선에서 가쪽눈구석 수평면과 큰광대근, 작은광대근 간의 평균 거리는 각각 20.0 mm, 17.9 mm, 22.8 mm, 20.8 mm 로 측정되었다. 각 수직면에서 눈둘레근과 표피 간의 평균 거리는 각각 4.9 mm, 4.8 mm, 5.5 mm, 4.7 mm 로 나타났다. 또한 각 수직면에서 큰광대근, 작은광대근과 눈둘레근 간의 평균 거리는 각각 3.0 mm, 3.1 mm, 4.5 mm, 4.1 mm 로 측정되었다.

본 연구의 결과는 초음파와 Sihler 염색법을 통해 얻은 해부학적 정보를 바탕으로 눈가주름 보톨리눔독소 주사에 대한 새로운 해부학지식을 제안한다. 또 임상에서 보툴리눔독소 주사 시 합병증을 최소화하고 주사 효과를 향상시키는 데 기여할 것으로 판단된다.

핵심되는 말 : 눈둘레근, 초으파, Sihler염색, 눈가주름, 보툴리눔독소